Chapter 2

# Application of artificial neural networks and UAV-based air quality monitoring sensors for simulating dust emission in quarries

Long Quoc Nguyen[a,b], Luyen K. Bui[a,c], Cuong Xuan Cao[a], Xuan-Nam Bui[b,d], Hoang Nguyen[b,d], Van-Duc Nguyen[b,e], Chang Woo Lee[e], and Dieu Tien Bui[f]

[a]*Faculty of Geomatics and Land Administration, Hanoi University of Mining and Geology, Hanoi, Vietnam,* [b]*Innovations for Sustainable and Responsible Mining (ISRM) Research Group, Hanoi University of Mining and Geology, Hanoi, Vietnam,* [c]*Geodesy and Environment Research Group, Hanoi University of Mining and Geology, Hanoi, Vietnam,* [d]*Department of Surface Mining, Mining Faculty, Hanoi University of Mining and Geology, Hanoi, Vietnam,* [e]*Department of Energy and Mineral Resources, College of Engineering, Dong-A University, Busan, Republic of Korea,* [f]*GIS Group, Department of Business and IT, University of South-Eastern Norway, Bø i Telemark, Norway*

## 1 Introduction

### 1.1 Motivations

As one of Vietnam's most important economic activities, the mining industry has been developing at a high pace. Stone, limestone, and rock are the most common construction materials in high demand due to rapid urbanization. This results in a significant increase in the number of quarries in many regions. To meet the demand for construction, the production of quarries has been supported by the continuous application of advanced technologies. It is essential to continuously enhance the technology of all producing states to achieve all goals of mining production. Mine surveying and environmental management are among the essential activities that have received significant attention from mining managers and scientists.

The mining industry has made a significant contribution to the Vietnam economy. However, this industry also inevitably leads to many environmental problems. In Vietnam, larger-scale open-pit mines are mainly located near

**Applications of Artificial Intelligence in Mining and Geotechnical Engineering**
**https://doi.org/10.1016/B978-0-443-18764-3.00012-6**

populated areas. For example, Tan My and Thuong Tan are among the largest stone quarries in Vietnam, just several kilometers from Tan Uyen town, Binh Duong province. While blasting is an integral part of open-pit mining, it usually causes the emission of particulate materials, for example, dust pollution and gasses potentially hazardous to health [1]. Blasting usually results in airblasts, ground vibration, fly rock, toxic fumes, and particulate matter (PM). All blasting events in mining areas emit the primary residue of PM [1], for example, $PM_{1.0}$, $PM_{2.5}$, and $PM_{10}$. To properly manage air quality in mining areas, it is crucial to establish an effective air quality monitoring system. To meet the high demand for construction materials, mine extension is inevitable. However, the expansion of a quarry is often considered with its potential environmental impacts. An air quality monitoring system can provide important data for the environmental management of quarries not only at present but also in the future when these quarries are expanded.

## 1.2 Related works

Recently, the rapid development in the unmanned aerial vehicle (UAV) technology has brought many benefits to a wide range of military and civil fields, such as logistics and transportation [2,3], precise agriculture [4,5], forest management and biodiversity conservation [6], hazardous and environmental management [7], and urban management [8–10]. The preliminary successes of UAV applications have proved that this technology could be promising and likely to be employed in the broader field. While the world has witnessed many excellent examples of using UAV technology in the mining industry for topographical surveys, safety investigations, and other works [11], this technology is still relatively new to Vietnam [12]. For instance, UAV technology was used to conduct a topographic survey of slope areas on an open-pit mine [13].

Another UAV-based topographic survey of an ore stockpile was given by Cryderman et al. [14]. These authors used topographic data to estimate ore carrying capacity. Lee and Choi [15] have proved that fixed-wing and rotary-wing UAVs, the most popular ones, can be used effectively in both small-scale and large-scale open-pit mines as a topographic surveying tool [15]. For air quality monitoring in open-pit mine sites, results of the laboratory and field tests conducted by Alvarado et al. [1] demonstrated the feasibility of coupling an optoelectronic dust sensor with UAVs.

In recent years, UAV-based systems have been considered for monitoring dust pollution, including particulate matter $PM_{1.0}$, $PM_{2.5}$, and $PM_{10}$ [16–18]. DJI Matrice 600 Pro with six propellers may be the most popular used due to the ability to carry a payload of up to 6 kg [19,20]. However, the price of more than 5000 USD and relatively large weight ($>10$ kg) when carrying is a hindrance when applying to open-pit mines. Thus, lighter weight UAV-based systems, that is, Inspire 2, should be investigated. In addition, predicting $PM_{1.0}$, $PM_{2.5}$, and $PM_{10}$ play a vital role in the pollution assessment. The literature review shows that machine learning, that is, support vector machines [21], neural networks

[22], and deep learning [22] are state-of-the-art methods used. Nevertheless, applications of machine learning for dust pollution prediction are still rare.

### 1.3 Contributions

As mentioned above, the application of UAVs has been proven as an alternative tool for air quality monitoring. In this study, a low-cost UAV-based system was employed at Tan My and Thuong Tan quarries in Binh Duong province, one of southern Vietnam's largest groups of stone quarries. This low-cost UAV system, named as UMS-AM, is designed to collect a variety of data that can be used for optimizing mining operations and control the atmospheric environment. Herein, we focus on monitoring the atmospheric environment at the quarries using the UMS-AM; how the multilayer perceptron neural network (MLP neural nets) could be used to predict three dust pollution, $PM_{1.0}$, $PM_{2.5}$, and $PM_{10}$, and finally, generating 3D model for $PM_{1.0}$, $PM_{2.5}$, and $PM_{10}$.

## 2 Proposed UMS-AM system

### 2.1 UAV platform

UAVs are classified based on different but interrelated characteristics such as size and payload, wing types, flight endurance, flight range, altitude, and capabilities [23]. With the wing types, there are two main subtypes, namely, the rotary-wing and fixed-wing UAVs. The latter is suitable for applications with longer flight endurance, but large space is needed for take off and landing. Although the former uses batteries and has shorter flight times [6], it has been increasingly common because of its ability to take off and land vertically in a small space and to maintain position. Therefore, in this study, a rotary-wing UAV was considered a feasible platform for the system. Specifically, its characteristics are given in Table 1.

**TABLE 1** Main parameters of the Inspire 2 used in this study.

| No. | Parameter | Inspire 2 |
|---|---|---|
| 1 | Weight | 4000 g |
| 2 | Battery | 4280 mAh |
| 3 | Camera | Multi: CMOS, 1″ 20 MP |
| 4 | Max flight time | Approx. 27 min |
| 5 | Cruise speed | – P-mode/A-mode: 16.4 ft./s (5 m/s)<br>– S-mode: 19.7 ft./s (6 m/s) |
| 6 | Radio link range | 7 km |
| 7 | Payload | Approx. 1.9 kg |

Various UAVs are currently available for the mining industry; however, low price is still considered the main issue. Furthermore, the payload is also a critical issue for this study because several air quality sensors and accessories are mounted on the UAV. For this purpose, DJ Inspire 2 (Fig. 1) was considered to use.

**FIG. 1** DJI Inspire 2. *(https://www.dji.com)*

## 2.2 Sensor networks

### *Optical sensors (Inspire 2's camera parameters)*

The DJI Inspire 2 is equipped with Zenmuse X4S, a powerful camera featuring a 20-megapixel 1-in. sensor. Dynamic range is increased from the Zenmuse X3 by one stop, with the signal-to-noise ratio and color sensitivity increased by 1.5 stops for next-level image quality. The Zenmuse X4S uses a DJI-designed compact lens with low dispersion and low distortion 24 mm equivalent prime lens. This 84° FOV high-resolution lens make the Zenmuse X4S powerful during aerial imaging as it is on the ground. Combined with CineCore 2.0 and the Inspire 2's powerful image processing system, the camera can record 4 K/60H.264 and 4 K/30H.265 videos at a 100 Mbps bitrate and an oversample 5.2 K video into 4 K video in real-time, capturing fine image details. Furthermore, in Burst Mode, the Zenmuse X4S supports 14 fps shooting at 20 megapixels in both JPEG and DNG formats, hence the balance between agility and image quality (https://www.dji.com/zenmuse-x4s).

In this study, together with the Zenmuse X4S, we used other sensors to measure various kinds of toxic gasses in the air, including carbon monoxide (CO), nitric oxide (NO), nitrogen dioxide ($NO_2$), sulfur dioxide ($SO_2$), and dust with $PM_{2.5}$, $PM_{10}$. In particular, the sensors from Alphasense, including CO-B4, NO-B4, $NO_2$-B43F, and $SO_2$-B4 were used to measure the toxic gas. Most sensors use individual sensor boards (ISBs) with four electrodes to convert the ADC signals with 12-bit. To measure the toxic gas, ISB uses the ADC chip to measure very small amounts of current and converts it into one part per million (ppm) of gas concentration. For example, CO-B4 has a 2.000 maximum ppm and converts the current in the range from 420 to 650 nA at 2 ppm. NO-B4 has its sensitivity from 500 to 850 nA at 2 ppm and 50 of maximum ppm. $NO_2$-B43F converts from −200 to −650 nA at 2 ppm and has 50 of

maximum ppm. $SO_2$-B4 measures and converts 275–520 nA at 2 ppm and has 200 maximum ppm.

The B4 series (four-electrode sensors) provides OEMs with reliable sensors for several high-volume applications, especially air quality networks requiring shallow parts per billion (ppb) detection levels. Intense signal levels combined with low zero current allow the resolution to $<10$ (ppb) and a wide operating range. The sensors are suitable for fixed installation sensing heads, portable safety instruments, urban/indoor air monitoring, and stack gas analyzers. In addition, the B4 sensor series offers our electrolyte leak-free guarantee and reliable long-term detection performance. The leak-proof housing is molded with a color-coded top for ease of identification.

Fig. 2 shows a simplified schematic of an electrochemical sensor measurement circuit. Electrochemical sensors allow gas to diffuse into the sensor through a membrane and interact with the working electrode (WE). The sensor reference electrode (RE) provides feedback to maintain a constant potential with the WE terminal by varying the voltage at the counter electrode (CE). The direction of the current at the WE terminal depends on whether the reaction occurring is oxidation or reduction. In the case of carbon monoxide, oxidation occurs; therefore, the current flows into the working electrode, which requires the counter electrode to be at a negative voltage (typically 300–400 mV) for the working electrode. Therefore, the op-amp driving the CE terminal should have an output voltage range of approximately $\pm 1$ V concerning $V_{\mathrm{REF}}$ to provide sufficient headroom for operation with different types of sensors (Alphasense Application Note AAN-105-03, Designing a Potentiostatic Circuit, Alphasense, Ltd.).

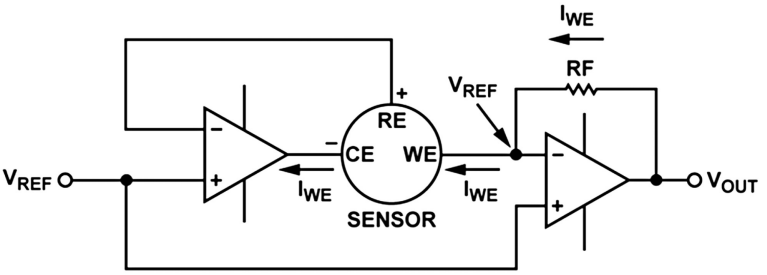


**FIG. 2** Simplified electrochemical sensor circuit.

The sensor PMS5003, which can measure dust from 0.3 to 10 μm, was used for the dust measurement. It uses serial communication (e.g., transport protocol with baud rate 9600 bps, one stop bit, and none-check bit) with TTL at level 3.3 V to transmit data to Microcontroller. PMS5003 is a digital and universal particle concentration sensor, which can be used to obtain the number of suspended particles in the air, that is, the concentration of particles, and output them as a digital interface. In addition, this sensor can be inserted into variable instruments related to the concentration of suspended particles in the air or other environmental improvement equipment to provide correct concentration data in time.

The laser scattering principle is used for such sensors, that is, produce scattering by using the laser to radiate suspending particles in the air, then collect scattering light to a certain degree, and finally obtain the curve of scattering light change with time. Finally, the equivalent particle diameter and the number of particles with different diameters per unit volume can be calculated by a microprocessor based on the MIE theory. The functional block diagram of the dust sensor is shown in Fig. 3.

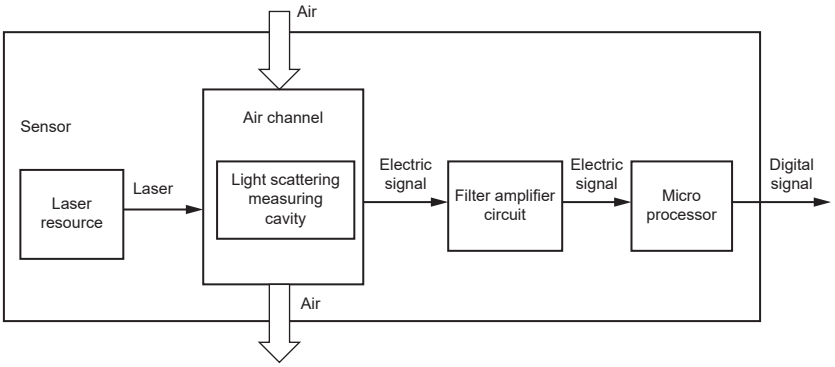


**FIG. 3** Functional block diagram of the dust sensor.

### *Air quality monitoring system*

To evaluate the air quality of the deep pit mine in this study, three dust pollutants, $PM_{1.0}$, $PM_{2.5}$, and $PM_{10}$ were measured. Table 2 shows the primary descriptions of the sensors used in this study. Due to the load limitation of UAVs, light and compact sensors were packed in a perforated box and mounted on the vehicle. Fig. 4 shows the monitoring box installation and a picture of the UAV flight. The communication link plays an essential role between data collection and transmission. The data transmission should satisfy the stability and reliability requirements when the UAV equipped with the monitoring sensor box reaches a high altitude. Thus, a smartphone or a tablet was attached to the monitoring box as a relay station and also a transceiver to store the measurement data. The structure of the UAV air quality monitoring platform and the system concept are illustrated in Fig. 4. In this study, before flying the UAV, all the sensors were calibrated.

**TABLE 2 The specifications of the air quality monitoring sensors used in this study.**

| Parameters | Sensor category | Range | Precision | Resolution |
|---|---|---|---|---|
| $PM_{10}$ | Laser dust sensor | 0–500 μg/m$^3$ | ±10% | 0.3 μg/m$^3$ |

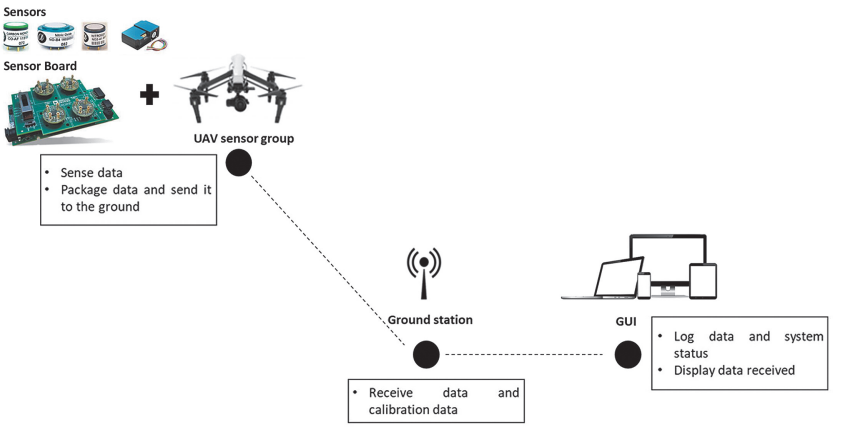


**FIG. 4** The structure of the UAV-based air quality monitoring platform used in this study.

## *Communication and networking subsystems*

### Packaging the data from the sensor to send to the ground station

For transmitting the data from the sensors to the ground station, the microcontroller compressed the data of all sensors into the packages with Modbus RTU protocol and sent it to the ground station via LoRa (long-range) technology at 490 MHz of radiofrequency. In addition, the data are backed up to the memory card in real-time to avoid losing data due to the disconnection between the measurement and ground stations.

### Hardware interconnection

To facilitate the interconnections across the modules, we first embedded a system capable of receiving data packages from the dust sensors via serial communication, such as SPI, RS232/RS485/422, and I2C. Then, we encapsulate these data into the Modbus RTU protocol before transmitting it to the ground station.

First, a LoRa transceiver module with 490 MHz transmit radiofrequency is connected to the measurement device to transmit the Modbus RTU package to the ground station. Second, at the ground station, we used the LoRa gateways to collect data transmitted from multiple measurement devices (mobile, fixed stations) to transmit these data packages to the monitoring and analyzing program designed and installed on the computers at the ground station in real-time. Also, within the data package, we identify the measurement devices with a unique code that allows the gateways to recognize the signal transmitted from the measuring devices with the corresponding code. Then, the real-time monitoring and analyzing program can distinguish each measuring device's data. Finally, two ground monitoring stations were installed on the top of the pit mainly to monitor the atmospheric condition of the free stream, including the barometric pressure, temperature, wind velocity, and direction.

In this study, the real-time monitoring of measurement results was considered. Herein, the data transmission directly to the ground station allows monitoring and tracking of the change in the air quality during the measurement time. In addition, at mobile and fixed measurement stations, the data are backed up to the memory card in real-time to avoid losing data due to the disconnection between the measurement and ground stations. This storage allows data to be instantly updated to the ground station when connected again to avoid data interruption during monitoring. We used two methods simultaneously in the data storage process.

## 3 Study site

Tan My and Thuong Tan (Fig. 5) are the largest group of quarries in southern Vietnam. These stone quarries cover an area of around 12 $km^2$ and provide hundreds of thousand tons of stone per year to southern Vietnam's construction. The depth of these quarries ranges from around 70 to 100 m. Dust from mining


**FIG. 5** Location of the Tan My and Thuong Tan quarries.

areas can irritate the eyes, skin, and respiratory tract, and prolonged exposure can lead to a range of serious lung diseases including silicosis, coal workers' pneumoconiosis (CWP), chronic obstructive pulmonary disease (COPD), and lung cancer.

## 4 Data monitoring measurement and methodology

### 4.1 Air quality monitoring measurement

This study focuses on the two research objectives: (1) Monitoring the atmospheric environment at the quarries using the UMS-AM and (2) predicting the density of air components using MLP neural nets. In deep pit stone quarries, pollutant dispersion depends on the surface wind as well as the air density differences between the inside and outside of the pit. The UAV has less flying time with more load due to the limited battery capacity. Herein, the total load, including sensors and other accessories, is 1.0 kg, and the flying time is about 25 min. However, the flying time was shortened to 15 min due to the time for starting and landing.

Fig. 6 shows the UAV flight paths to measure the atmospheric environment within the pit. The space within the pit was divided into two sections: H1 at 45 m and H2 at 20 m, as shown in Fig. 6. UAVs systematically flew through these zones. Finally, the collected data were utilized to make 3D dust maps.

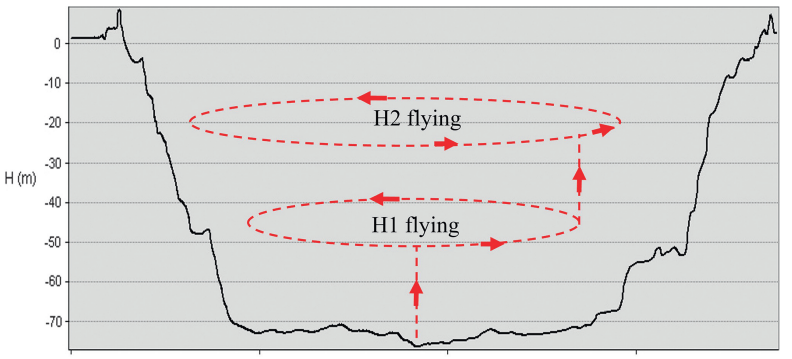


**FIG. 6** UAV flight paths to measure the atmospheric environment at a quarry.

In this study, a total of 879 points were collected by UMS-AM. As dust is considered a main pollutant generated by the production of quarries, the results of monitoring dust within the quarry included $PM_{1.0}$, $PM_{2.5}$, and $PM_{10}$ are given in Table 3.

**TABLE 3** Statistics of measurement data.

| Statistical values | Latitude $X$ (°) | Longitude $Y$ (°) | Altitude $H$ (m) | $PM_{1.0}$ ($\mu g/m^3$) | $PM_{2.5}$ | $PM_{10}$ |
|---|---|---|---|---|---|---|
| Mean | 11,043 | 106,881 | 24,641 | 18,912 | 25,661 | 27,451 |
| Standard deviation | 0.0008 | 0.0005 | 5590 | 6200 | 10,118 | 12,122 |
| Min | 11,042 | 106,880 | 2350 | 12 | 15 | 15 |
| Max | 11,045 | 106,882 | 30,350 | 60 | 84 | 108 |

## 4.2 Multilayer perception neural network

In this study, to predict the density of air components within the quarry when it is expanded in the future with larger production and a more immense ending depth, MLP neural nets was considered. We selected MLP neural nets because they can predict the outcome accurately.

Fig. 7 shows the structure of the MLP neural nets model in this study. The network consists of three layers: (1) The input layer with three neurons ($X$, $Y$, $H$), (2) the hidden layer has four sub-layers with a total of 56 neurons, and (3) the output layer contains three neurons ($PM_{1.0}$, $PM_{2.5}$, and $PM_{10}$). The activate function is sigmoidal that connects the input layer to the hidden layer,

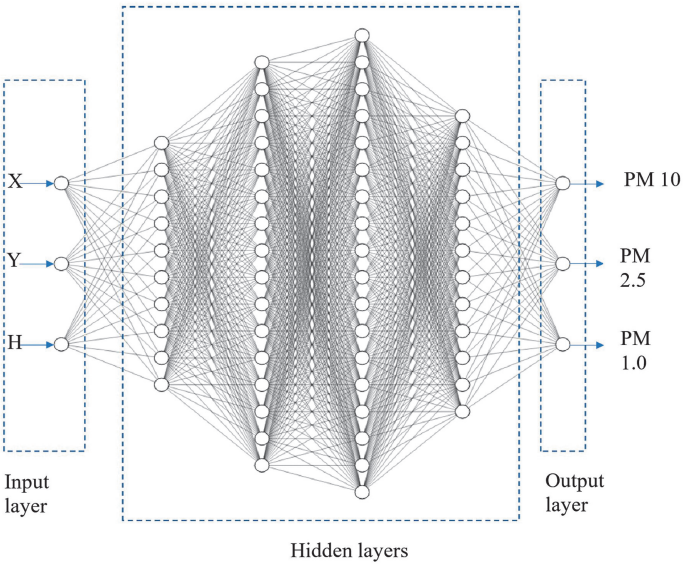


**FIG. 7** Structure of MLP neural nets used for predicting air components in this study.

whereas the purelin is used as the transfer function between the hidden layer and the output. The modeling process was carried out using the Neural Network Toolbox in the MATLAB 2019b software.

The MLP neural nets model receives information through its input layer via the activate functions before computing and transferring via each hidden layer. Finally, the results will be passed through the output layer. It is important to note that the outcomes of the MLP neural nets will depend on the training process. In this study, the training process was based on the supervised learning method with the input data and the requirement of output data. The input data of the model included the coordinates of UAV air observation points which were collected by a global navigation satellite system receiver mounted on the UAV. Around 80% of the dataset was used for training the model, and the remaining 20% of the dataset was used for validating the model's performance. Three parameters including $X$, $Y$, and $H$ are the input variables, and $PM_{1.0}$, $PM_{2.5}$, and $PM_{10}$ are the output variables.

## 5 Results

The exploitation is planned to end at −150 m below the ground level, and the quarry was designed based on this plan. To validate the performance of the proposed MLP Neural Nets model for predicting air quality in this research, the entire measured dataset is divided into a training dataset corresponding to 615 points (70%) and a validating dataset from the remaining 264 points (30%). The model was first trained based on the training dataset by which the parameters are estimated. The derived parameters are then applied to all points from both the training and validating datasets so that the validation is conducted by the difference between predicted and measured values, with the statistics (maximum, minimum, and mean values) provided in Table 4.

The maximum and minimum differences between predicted and monitored $PM_{1.0}$, $PM_{2.5}$, and $PM_{10}$ were found among [12–60] μg/m$^3$, [15–84] μg/m$^3$, and [15–108] μg/m$^3$, respectively. Fig. 8 compares MLP Neural Nets model-based

**TABLE 4** Statistics of the difference between predicted and measured PMs from the training and validating datasets (units: μg/m$^3$).

| Metrics | Training dataset (80%) | | | Validating dataset (20%) | | |
|---|---|---|---|---|---|---|
| *Statistics* | $PM_{1.0}$ | $PM_{2.5}$ | $PM_{10}$ | $PM_{1.0}$ | $PM_{2.5}$ | $PM_{10}$ |
| Maximum | 59 | 82 | 102 | 60 | 84 | 108 |
| Minimum | 12 | 15 | 15 | 12 | 15 | 16 |
| Mean | 18.85 | 25.72 | 27.56 | 19.05 | 25.49 | 27.2 |

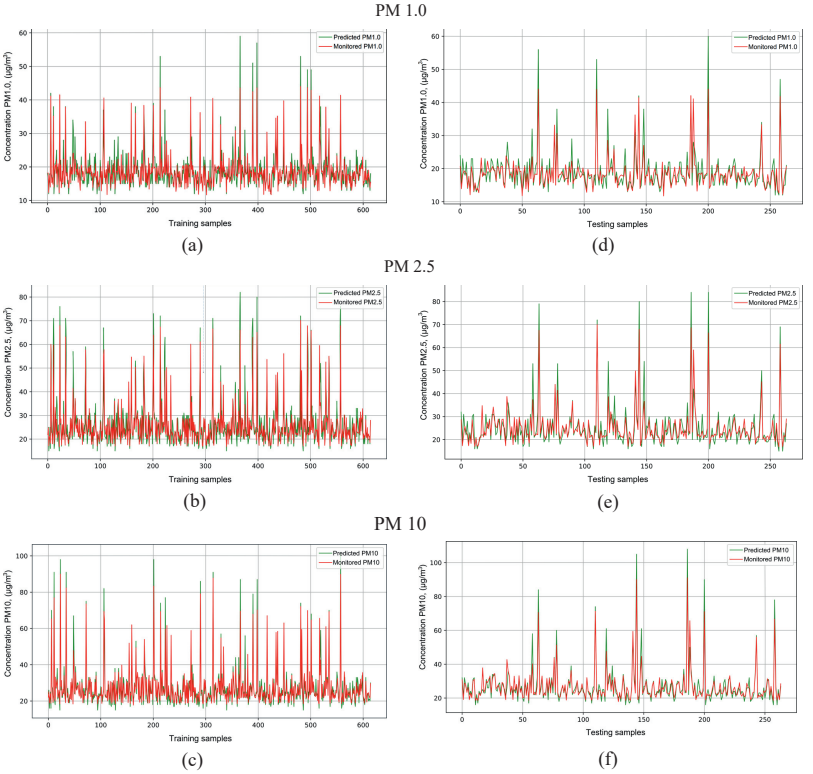


**FIG. 8** Comparisons between predicted and measured PM values from 80% training dataset (A–C) and 20% validating dataset (D–F).

predicted and measured values of PM1.0, PM2.5, and PM10 concentrations corresponding to the training (left) and validating (right) datasets, with corresponding correlations are shown in Fig. 9. The results indicate the values predicted when the quarry is excavated to the level of −150 m. Table 4 and Figs. 8 and 9 showed that the MLP neural nets have good performance in the prediction of dust concentrations.

To generate 3D air component models within the designed quarries, which is helpful in visualization of the air quality over the entire quarries, the Trilinear interpolation method [24] available in the Voxler software (https://www/goldensoftware.com) was used. Compared with other spatial interpolation methods, such as the nearest neighbor and natural neighbor, this method is the most suitable for spatial modeling of air components in a 3D space [18]. This method is linear interpolation with an extension of 3D space. Fig. 10 shows these 3D models generated for this study.

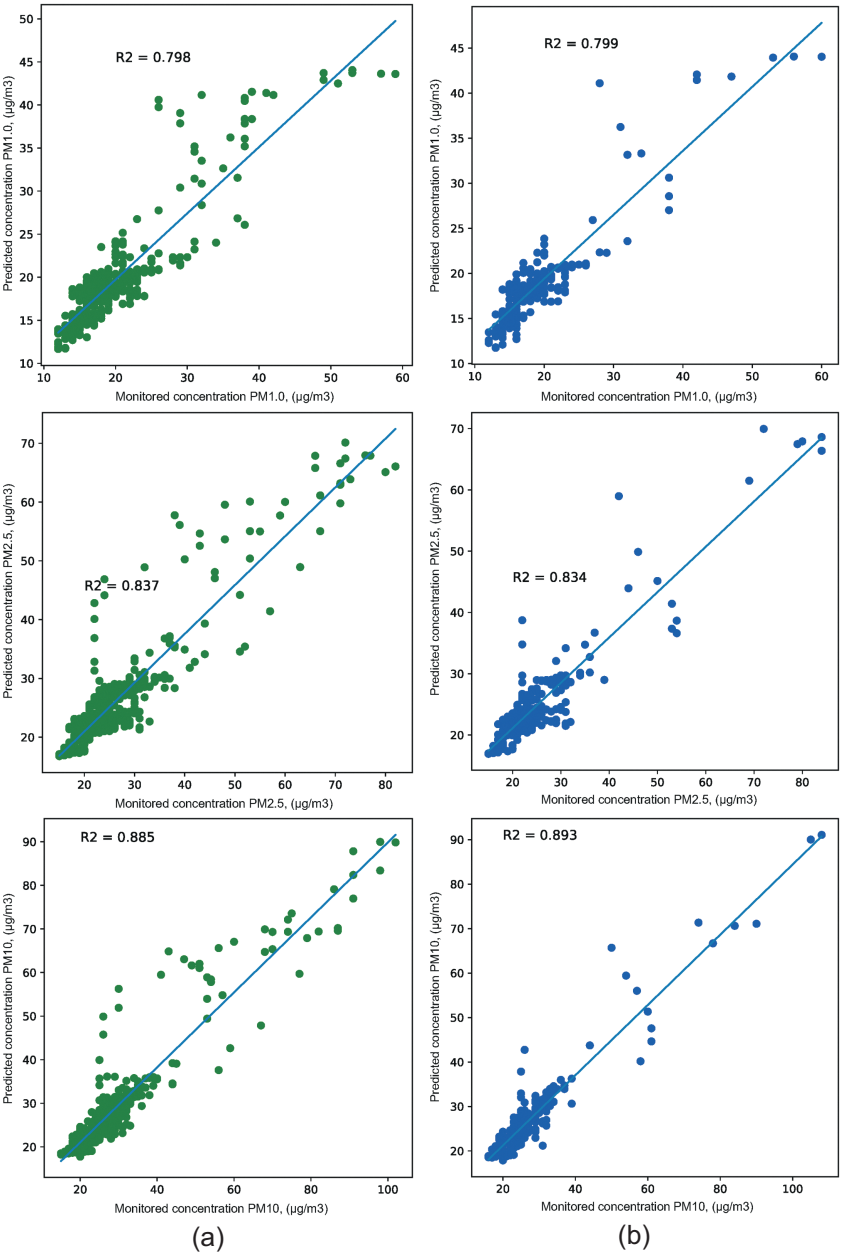


**FIG. 9** Correlation between predicted and monitored concentrations $PM_{1.0}$, $PM_5$, and $PM_{10}$. (A) Training dataset and (B) testing dataset.

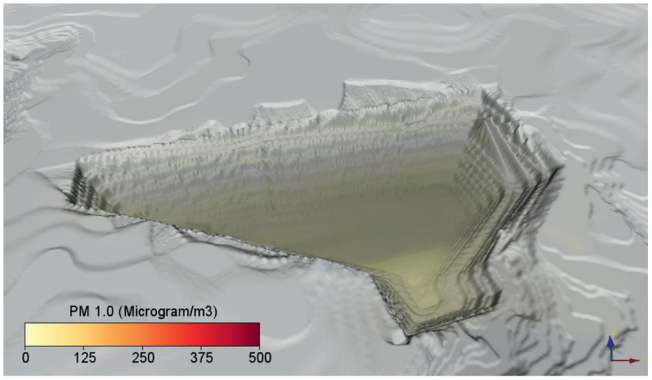


(a)

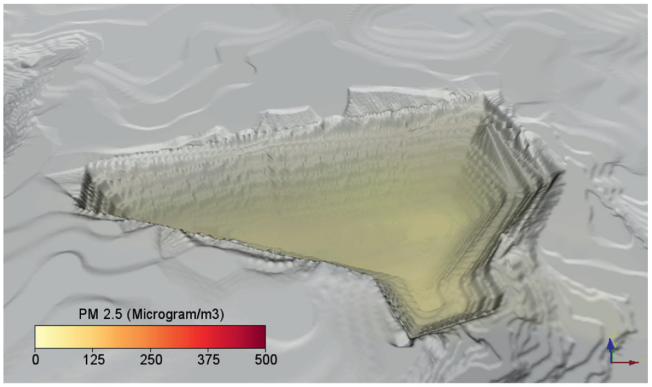


(b)

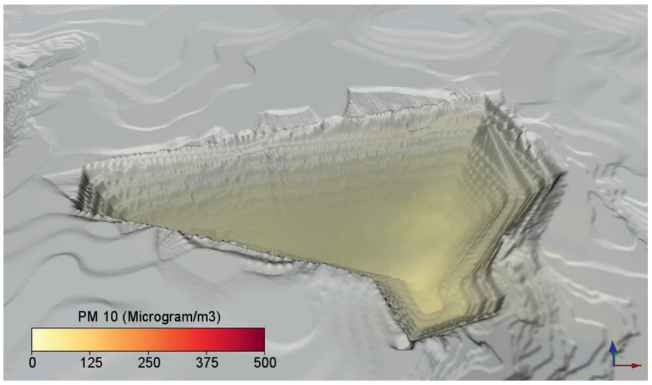


(c)

**FIG. 10** 3D dust models in the study quarries made by the MLP neural nets model: (A) $PM_{1.0}$, (B) $PM_{2.5}$, and (C) $PM_{10}$.

## 6 Conclusions

In this study, a UAV-based system has been developed ultimately for air quality management in the mining industry in Vietnam. The proposed UAV system included a DJI Inspire 2 equipped with an RGB Zenmuse X4S camera, air quality monitoring sensors, and a data logging system. Through the study site, the system proved to be a safe, effective, and economical tool for environmental management. Some of the limitations experienced during the study were closely related to the UAV system itself; the limitation on UAV allowable load was the most significant problem for monitoring purposes. One of the advantages of the low-cost UAV system is that the system equipped with low-cost, reliable sensors shows the applicability of the mine environment monitoring system within quarries. The MLP neural nets model can be used to predict the air component concentrations in time with an input dataset provided by the UAV-based system. Ultimately, the system can derive pollutant control measures since the air pollution profiles are visible in the 3D model.

## Conflicts of Interest

The authors declare no conflicts of interest.

## References

[1] M. Alvarado, F. Gonzalez, A. Fletcher, A. Doshi, Towards the development of a low cost airborne sensing system to monitor dust particles after blasting at open-pit mine sites, Sensors 15 (2015) 19667.

[2] L.A. Haidari, S.T. Brown, M. Ferguson, E. Bancroft, M. Spiker, A. Wilcox, et al., The economic and operational value of using drones to transport vaccines, Vaccine 34 (2016) 4062–4067.

[3] V. Olivares, F. Cordova, J.M. Sepúlveda, I. Derpich, Modeling internal logistics by using drones on the stage of assembly of products, Procedia Comput. Sci. 55 (2015) 1240–1249.

[4] V. Puri, A. Nayyar, L. Raja, Agriculture drones: a modern breakthrough in precision agriculture, J. Stat. Manag. Syst. 20 (2017) 507–518.

[5] C.A. Rokhmana, The potential of UAV-based remote sensing for supporting precision agriculture in Indonesia, Procedia Environ. Sci. 24 (2015) 245–253.

[6] J. Paneque-Gálvez, M.K. McCall, B.M. Napoletano, S.A. Wich, L.P. Koh, Small drones for community-based forest monitoring: an assessment of their feasibility and potential in tropical areas, Forests 5 (6) (2014) 1481–1507.

[7] S. Mourato, P. Fernandez, L. Pereira, M. Moreira, Improving a DSM obtained by unmanned aerial vehicles for flood modelling, in: IOP Conf. Series: Earth and Environmental Science, IOP Publishing, 2017.

[8] M.A. Khan, W. Ectors, T. Bellemans, D. Janssens, G. Wets, UAV-based traffic analysis: a universal guiding framework based on literature survey, Transport. Res. Procedia 22 (2017) 541–550.

[9] G. Salvo, L. Caruso, A. Scordo, Urban traffic analysis through an UAV, Procedia Soc. Behav. Sci. 111 (2014) 1083–1091.

[10] S. Spanogianopoulos, Q. Zhang, S. Spurgeon, Fast formation of swarm of UAVs in congested urban environment, IFAC PapersOnLine 50 (2017) 8031–8036.
[11] S. Lee, Y. Choi, Reviews of unmanned aerial vehicle (drone) technology trends and its applications in the mining industry, Geosystem Eng. 19 (2016) 197–204.
[12] T.D. Bui, C.V. Nguyen, M.H. Hoang, B.P. Dong, V.H. Nhu, T.A. Tran, et al., Xây dựng mô hình số bề mặt và bản đồ trực ảnh sử dụng công nghệ đo ảnh máy bay không người lái, in: Hội nghị khoa học: Đo đạc bản đồ với ứng phó biến đổi khí hậu, Hà Nội, 2016.
[13] T. McLeod, C. Samson, M. Labrie, K. Shehata, J. Mah, P. Lai, et al., Using video acquired from an unmanned aerial vehicle (UAV) to measure fracture orientation in an open-pit mine, Geomatica 67 (2013) 173–180.
[14] C. Cryderman, S.B. Mah, A. Shufletoski, Evaluation of UAV photogrammetric accuracy for mapping and earthworks computations, Geomatica 68 (2014) 309–317.
[15] S. Lee, Y. Choi, On-site demonstration of topographic surveying techniques at open-pit mines using a fixed-wing unmanned aerial vehicle (drone), Tunn. Undergr. Sp. 25 (2015) 527–533.
[16] A.M. Cárdenas, L.M. Rivera, B.L. Gómez, G.M. Valencia, H.A. Acosta, J.D. Correa, Pollution-and-greenhouse gases measurement system, Measurement 129 (2018) 565–568.
[17] R. Cichowicz, M. Dobrzański, Spatial analysis (measurements at heights of 10 m and 20 m above ground level) of the concentrations of particulate matter (PM10, PM2. 5, and PM1. 0) and gaseous pollutants (H2s) on the university campus: a case study, Atmos. 12 (2021) 62.
[18] L.Q. Nguyen, C.X. Cao, C.V. Le, B.N. Nguyen, T.A. Dang, T.Q. Le, et al., 3D spatial interpolation methods for open-pit mining air quality with data acquired by small UAV based monitoring system, Inżynieria Mineralna 1 (2020) 263–272.
[19] D. Huamanchahua, J.C. Huamanchahua, F. Fanny-Flores, Use of drones (UAVs) for pollutant identification in the industrial sector: a technology review, in: IEEE International IOT, Electronics and Mechatronics Conference (IEMTRONICS), 2022, IEEE, 2022, pp. 1–6.
[20] J. Jońca, M. Pawnuk, Y. Bezyk, A. Arsen, I. Sówka, Drone-assisted monitoring of atmospheric pollution—a comprehensive review, Sustainability 14 (2022) 11516.
[21] H. Madokoro, O. Kiguchi, T. Nagayoshi, T. Chiba, M. Inoue, S. Chiyonobu, et al., Development of drone-mounted multiple sensing system with advanced mobility for in situ atmospheric measurement: a case study focusing on PM2.5 local distribution, Sensors 21 (2021) 4881.
[22] S. Masoud, N. Mariscal, Y. Huang, M. Zhu, A sensor-based data driven framework to investigate PM 2.5 in the greater Detroit area, IEEE Sensors J. 21 (2021) 16192–16200.
[23] H.T. Berie, I. Burud, Application of unmanned aerial vehicles in earth resources monitoring: focus on evaluating potentials for forest monitoring in Ethiopia, Eur. J. Remote Sens. 51 (2018) 326–335.
[24] M. Sarmad, L.C. Ruspini, F. Lindseth, SIT-SR 3D: self-supervised slice interpolation via transfer learning for 3D volume super-resolution, Pattern Recogn. Lett. 166 (2023) 97–104.